Lessons Learned in Calorimetry at ATLAS

5th Terascale Detector Workshop

Sven Menke, MPP München

16. Mar 2012, Uni-Bonn

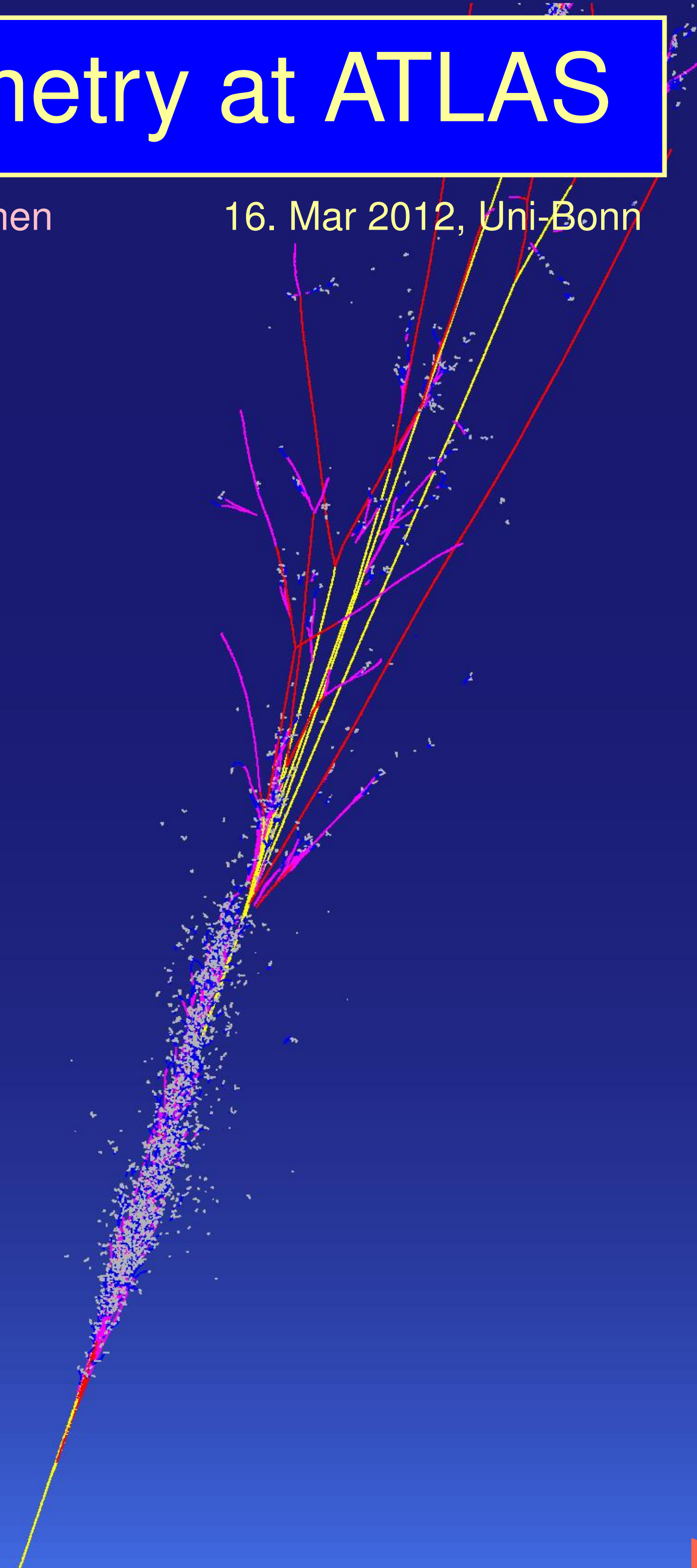

- ATLAS and the LHC
- Calorimetry in ATLAS
- Signal Reconstruction
  - from signals to cells
  - from cells to clusters
  - from clusters to jets
- Performance
  - Electrons and Photons
  - Jets
- Effects of PileUp
- Conclusions

ATLAS and the LHC

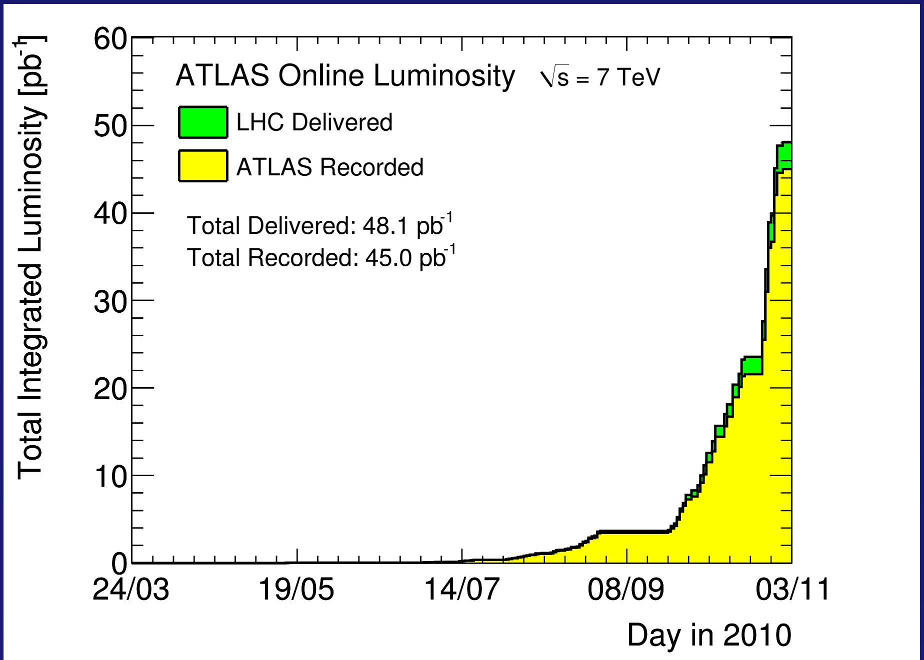

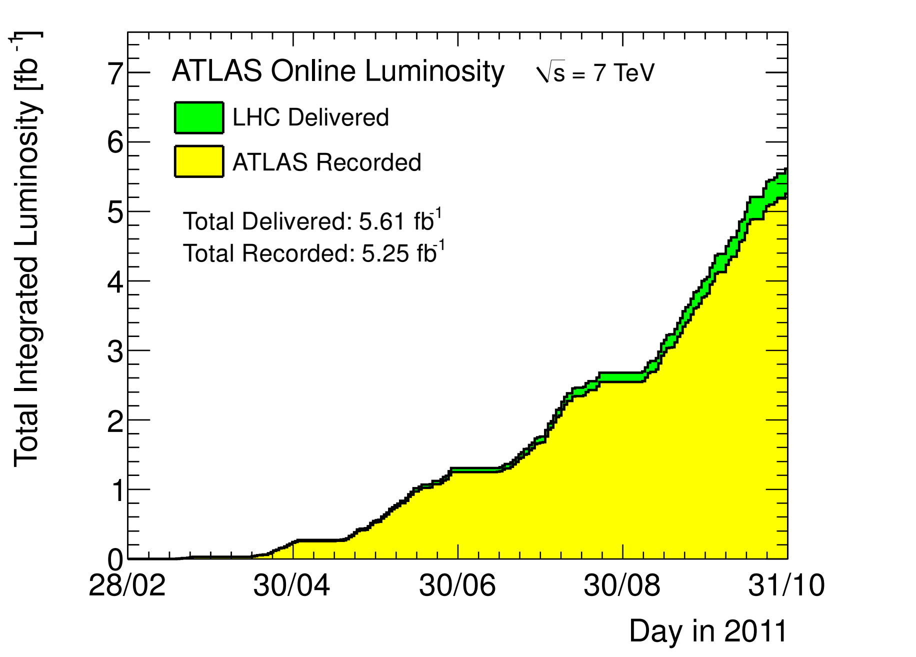

- LHC: pp Collisions @$\sqrt{s} = 7$ TeV since March 2010
- 2011 ATLAS recorded integrated luminosity @$\sqrt{s} = 7$ TeV: $L = 5.25\,\mathrm{fb}^{-1}$ as of 30-Oct-2011 (stop of pp-run)
- Bunch crossing distance in 2011: 50 ns
- Average number of interactions per bunch: $\langle\mu\rangle \simeq 6 - 12$

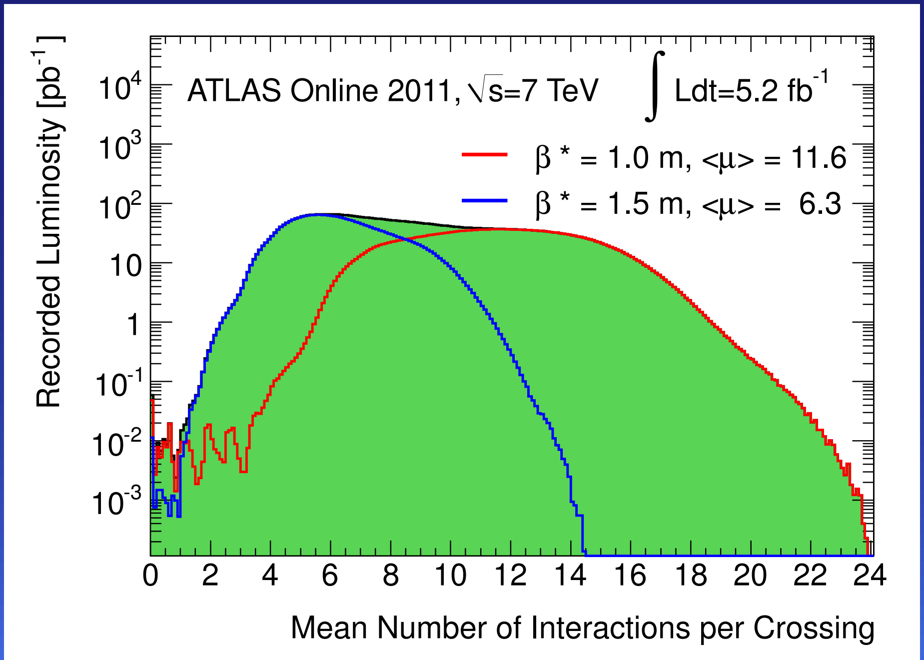

The ATLAS Detector

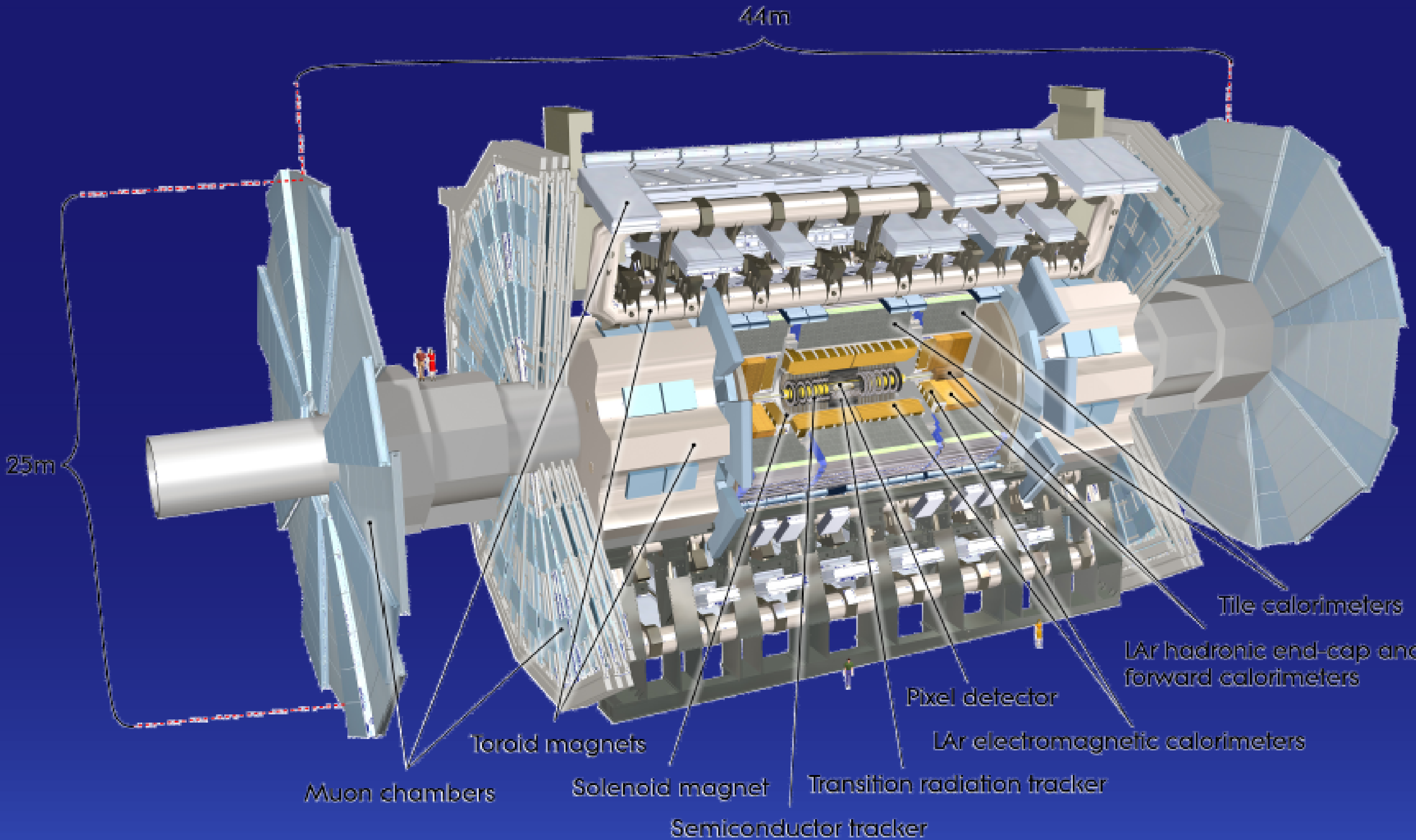

A Torodial **L**HC **A**paratu**S**: 25 m high; 44 m long; 7000 t heavy

ATLAS Calorimetry

- Electromagnetic Calorimeter: LAr/Pb Accordion sampling calorimeter
- Lead is the absorber to produce the secondary particles
- Liquid Argon in the absorber gaps is ionized and HV electrodes collect the current

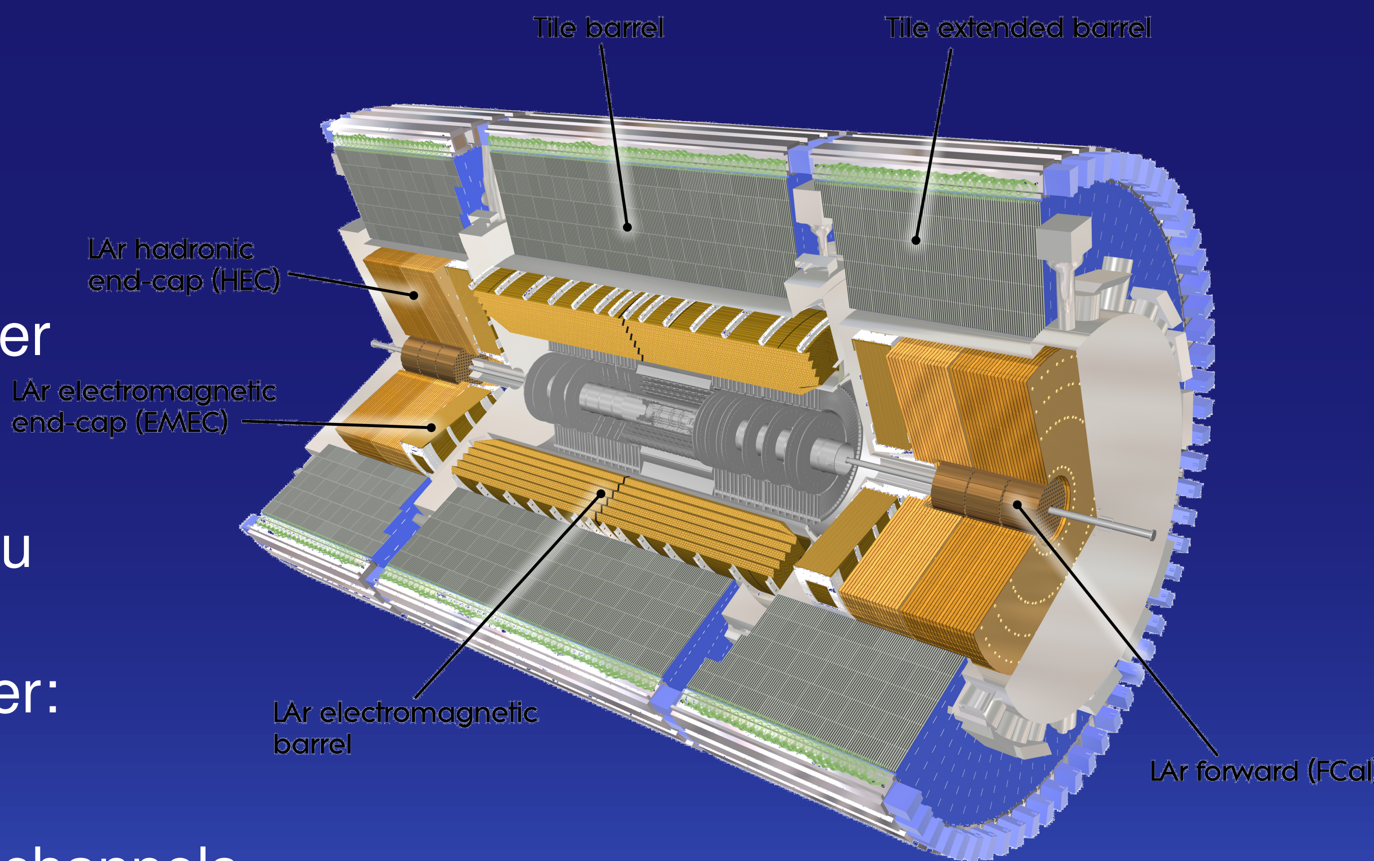

- Hadronic barrel calorimeter: Steel/Scintillator sampling calorimeter (Tile)
- Hadronic Endcap Calorimeter: LAr/Cu (HEC)
- Forward Calorimeter: LAr/Cu(W) (FCal)

- 190×10^3 readout channels
- Resolution for e/γ: $\sigma_E/E \simeq 10\%/\sqrt{E}$
- For jets: $\sigma_E/E \simeq 50\%/\sqrt{E} \oplus 3\%$

ATLAS Calorimetry ► LAr EM Calorimeter

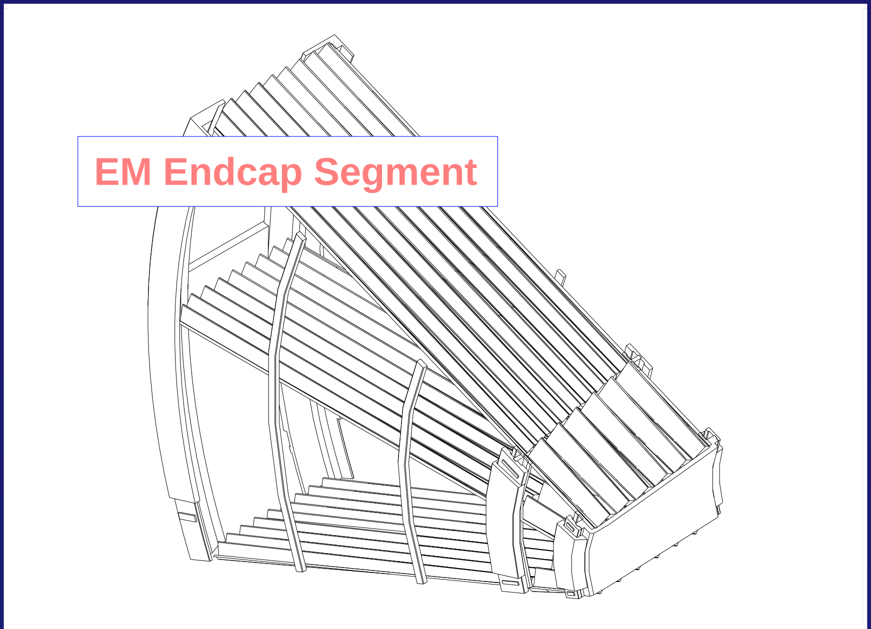

- EM absorber structure
  - Pb-Absorbers (1.5, 1.1, 1.7, 2.2 mm) arranged radially
  - Folding angle and wave height vary with r (End-cap)
  - Anodes pointing in η

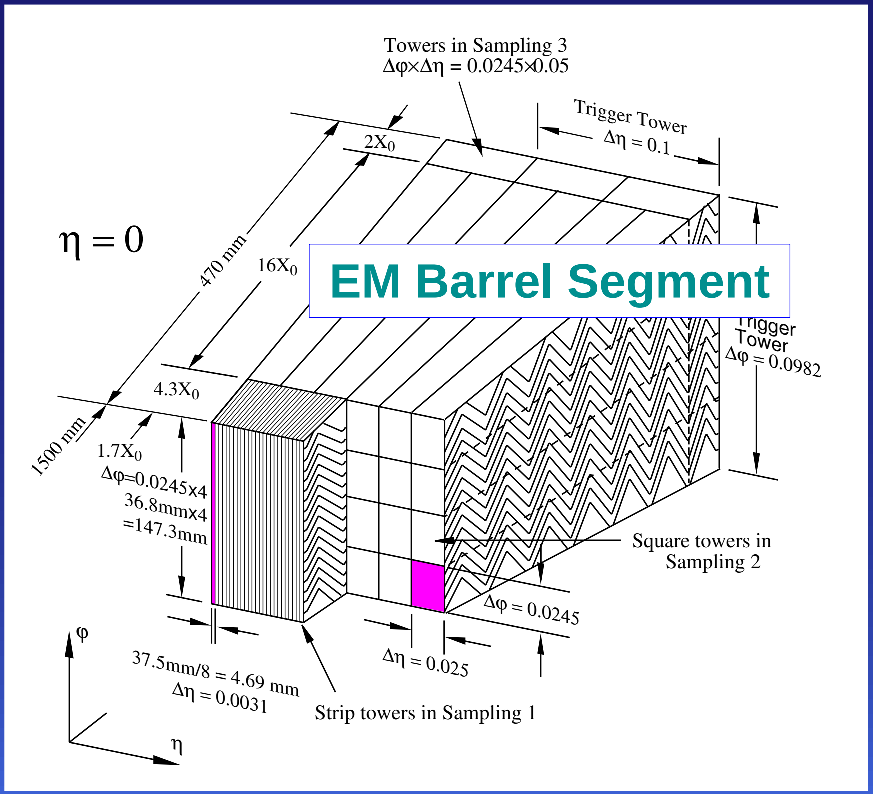

- EM readout structure
  - Layer1 (Front): $\simeq 2 - 4\ X_0$
    $\delta\eta \times \delta\phi = 0.025/8 \times 0.1$
  - Layer2 (Middle): $\simeq 16 - 18\ X_0$
    $\delta\eta \times \delta\phi = 0.025 \times 0.025$
  - Layer3 (Back): $\simeq 2 - 4\ X_0$
    $\delta\eta \times \delta\phi = 0.050 \times 0.025$
  - 173312 readout channels incl. PS

ATLAS Calorimetry ► Hadronic Tile Calorimeter

- Tile absorber structure
  - laminate of $4-5\,\mathrm{mm}$ thick steel plates (absorbers and spacers) stacked to $293.2\,\mathrm{mm}$ thick sub-modules
  - scintillating tiles are inserted in the holes left by the spacer plates
  - high periodicity makes absorber structure independent from optical instrumentation
  - 19 (9) sub-modules make one barrel (extended barrel) module
  - 64 identical modules in ϕ

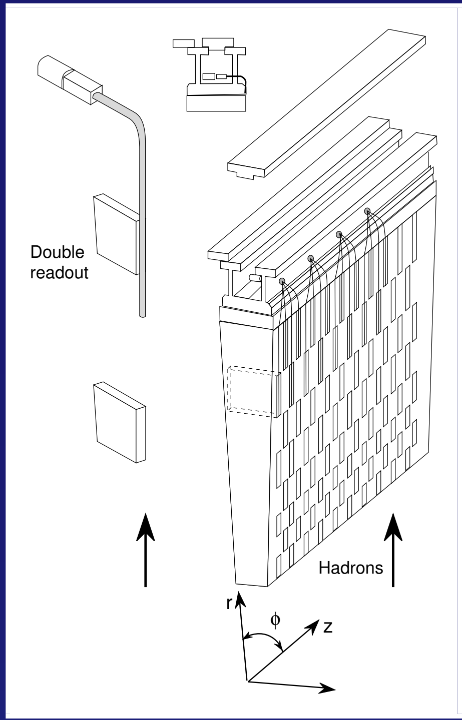

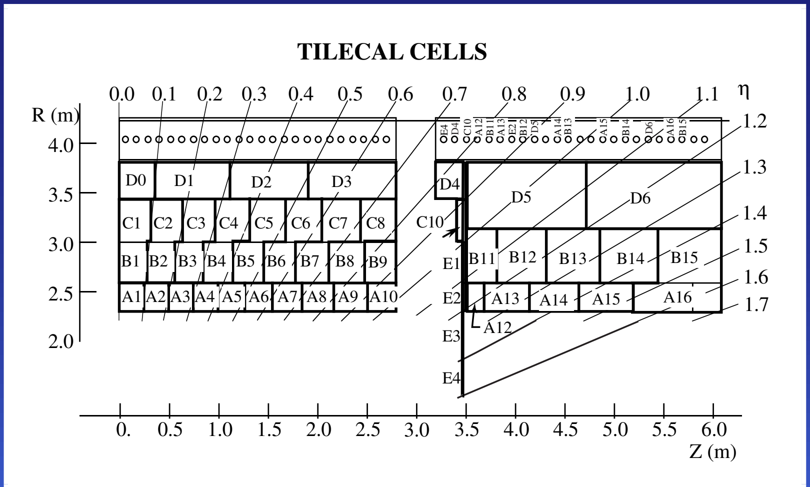

- Tile readout structure
  - tiles are grouped to readout cells in 3 longitudinal layers (B and C are readout together)
  - $\delta\eta \times \delta\phi \simeq 0.1 \times 0.1$ (0.2×0.1)
  - gap scintillators provide calorimetric information between TileB and TileEB and between EMB and EMEC
  - 5248 readout channels

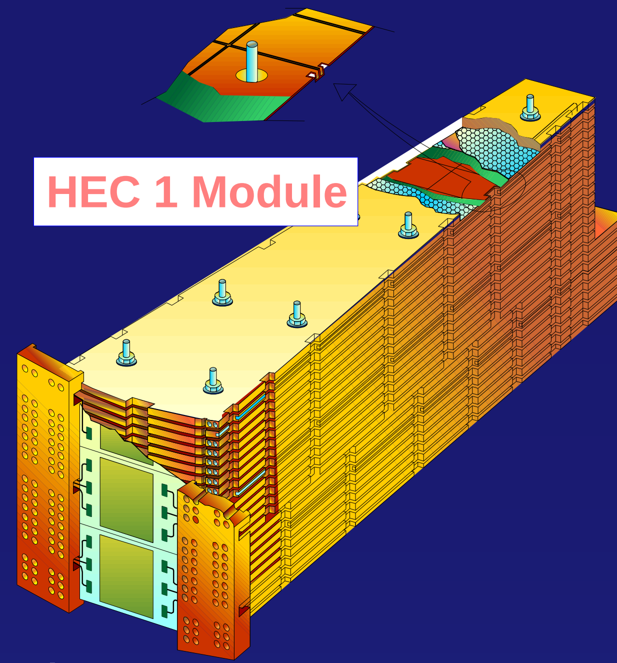

- HEC absorber structure
  - Absorbers plates parallel to beam axis
  - 2.5 cm thick Cu plates in HEC 1
  - 5.0 cm thick Cu plates in HEC 2

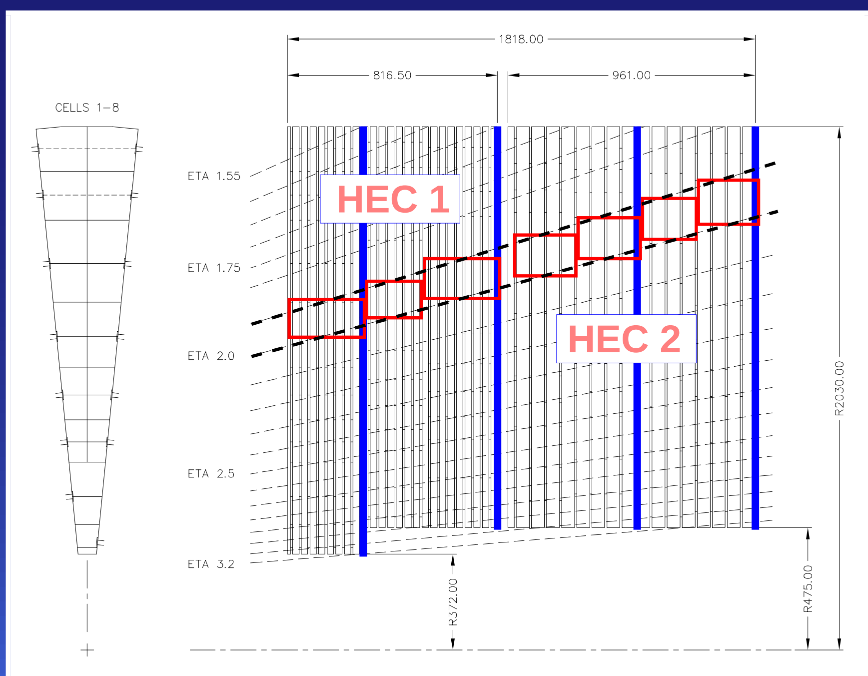

- HEC readout structure
  - $\delta\eta \times \delta\phi \simeq 0.1(0.2) \times 0.1(0.2)$
  - Layer1 (HEC1 Front): $\sum 8\,\text{gaps}$
  - Layer2 (HEC1 Back): $\sum 16\,\text{gaps}$ summed pseudo pointing in η
  - Layer3&4 (HEC2 Front&Back): $\sum 8\,\text{gaps}$ summed pseudo pointing in η
  - 5632 readout channels

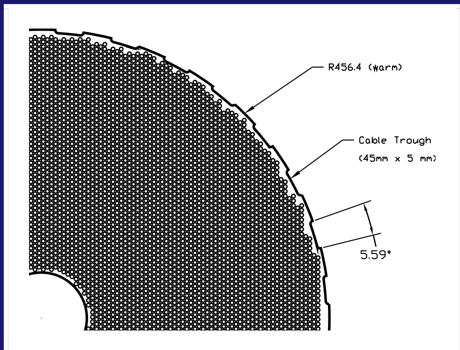

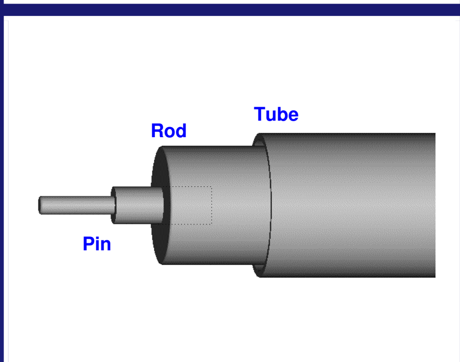

- FCal absorber structure
  - 3 modules made of 45 cm thick Cu (FCal1) or W (FCal2, FCal3)
  - 12260 (10200, 8224) holes in FCal1 (FCal2, FCal3) filled with electrodes consisting of an outer Cu tube and an inner Cu rod with 250 μm LAr gap between them
  - rods are centered inside the tubes by quartz fibres wound around the rods

- FCal readout groups
  - 2×2 (2×3, 3×3) tubes form one readout group
  - 1 (inner and outer border) or 2×2 (main part) readout group(s) form one readout channel
  - 3524 readout channels

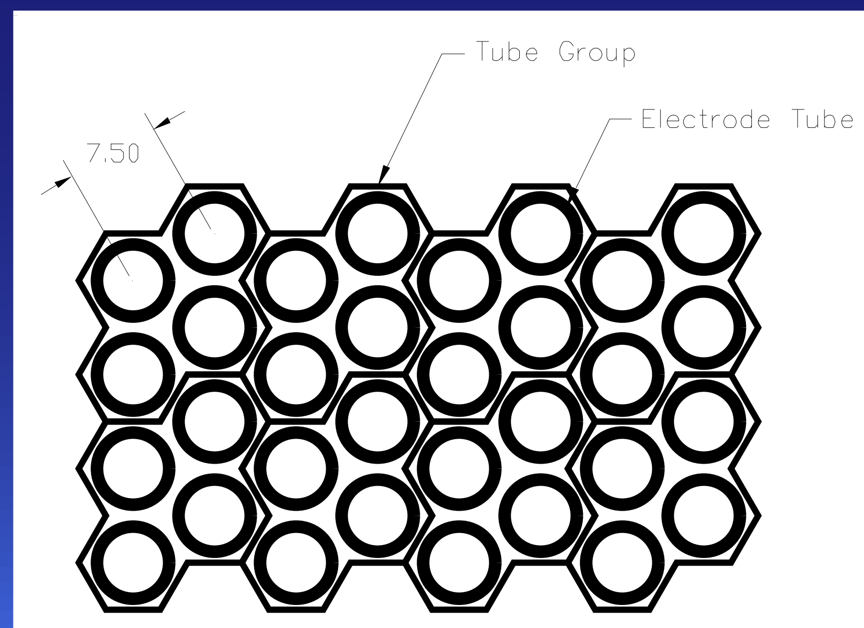

Electromagnetic vs. Hadronic Showers

- An electromagnetic shower
  - consists of visible EM energy only
  - is very compact ($X_0 \simeq 2$ cm)
  - can be simulated with high precision since mostly electromagnetic processes need to be calculated
  - allows high accuracy calibration (see talk by Stathes for details)
- A hadronic shower
  - consists of EM and hadronic energy (some invisible)
  - is very large ($\lambda_0 \simeq 20$ cm)
  - is difficult to simulate since it involves many QCD processes
  - limits the accuracy for calibration (mostly due to large fluctuations)
- The examples show 50 GeV showers of an electron (left) and a pion (right) in iron

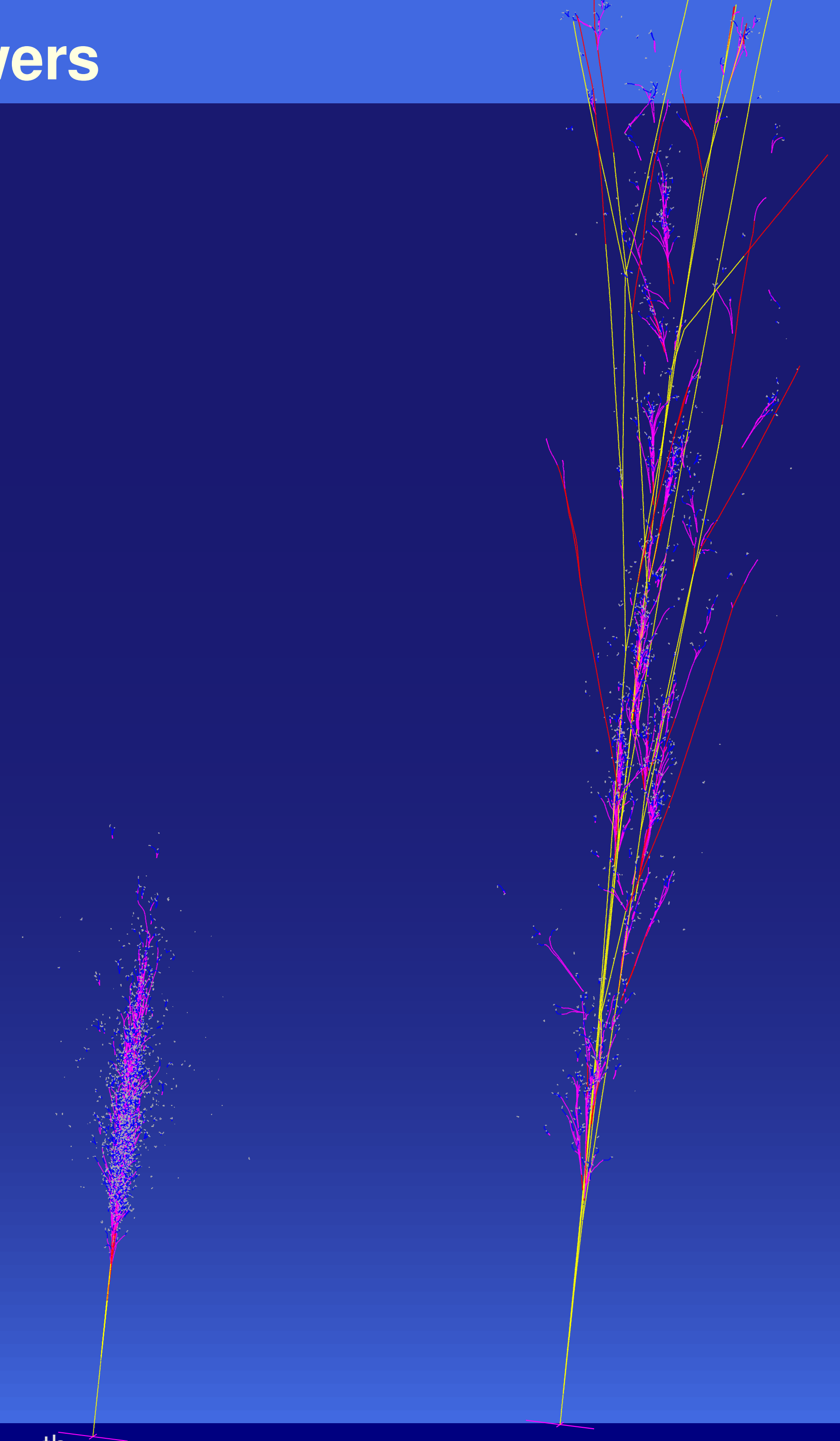

Hadron Calorimetry in ATLAS

- A hadronic shower consists of
  - EM energy (e.g. $\pi^0 \to \gamma\gamma$) $O(50\,\%)$
  - visible non-EM energy (e.g. $\mathrm{d}E/\mathrm{d}x$ from $\pi^\pm$,$\mu^\pm$, etc.) $O(25\,\%)$
  - invisible energy (e.g. breakup of nuclei and nuclear excitation) $O(25\,\%)$
  - escaped energy (e.g. ν) $O(2\,\%)$
- each fraction is energy dependent and subject to large fluctuations

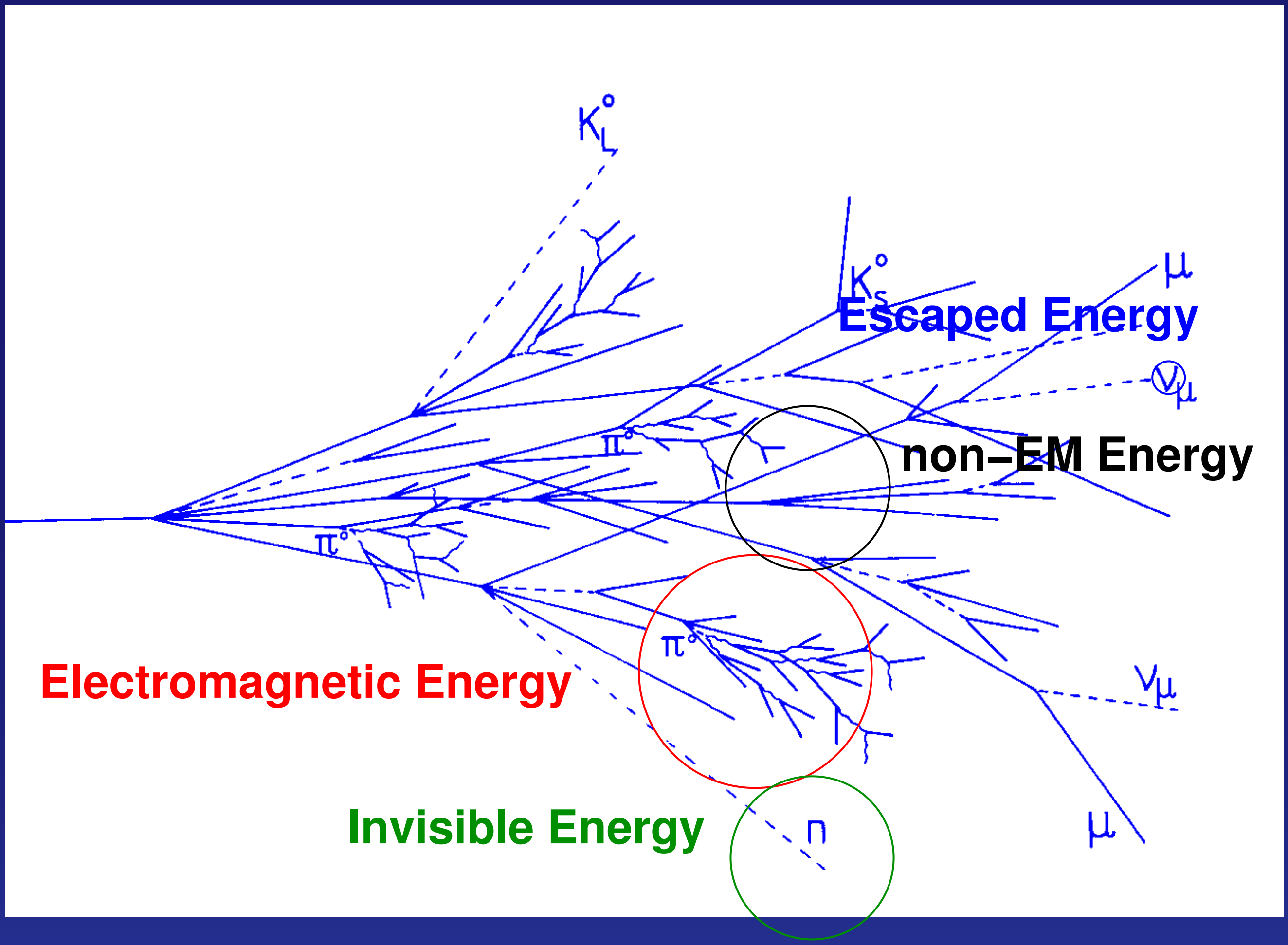

- invisible energy is the main source of the non-compensating nature of hadron calorimeters
- hadronic calibration has to account for the invisible and escaped energy and deposits in dead material and ignored calorimeter parts

- From a Geant4 simulation of EMEC and HEC:

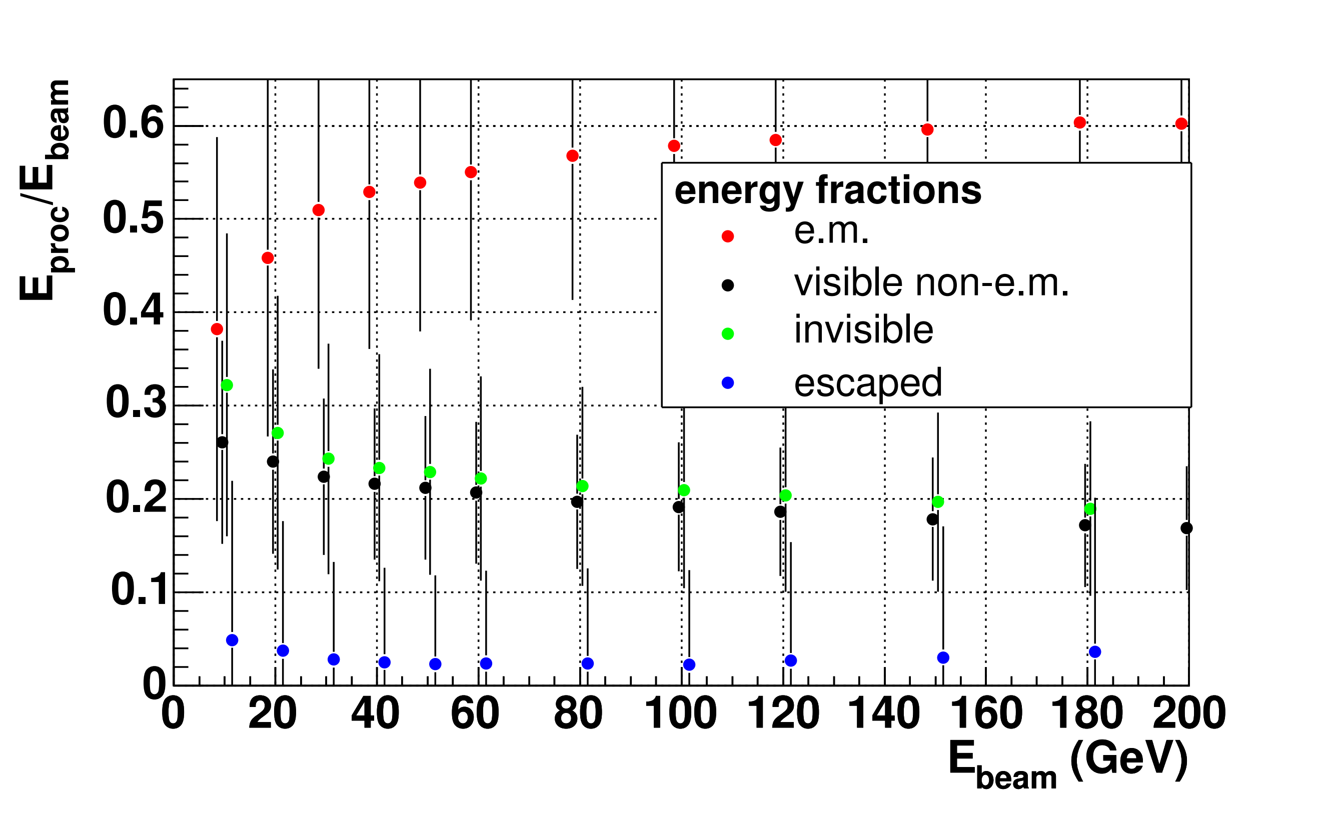

- EM energy strongly anti-correlated with visible non-EM energy
- visible non-EM energy strongly correlated with invisible energy

- need to separate EM part of the shower from the non-EM part
- apply a weight to the non-EM part to compensate invisible energy

- How to separate EM fraction from non-EM fraction?
  - $X_0 \ll \lambda \simeq 20\,\mathrm{cm}$
  - high energy density in a cell denotes high EM activity
  - low energy density in a cell corresponds to hadronic activity
  - apply weights as function of energy density

Calorimeter Reconstruction

- The cell is the smallest reco object
  - all ATLAS calorimeters together provide 187652 cells
  - each cell provides mainly the raw reconstructed energy in MeV

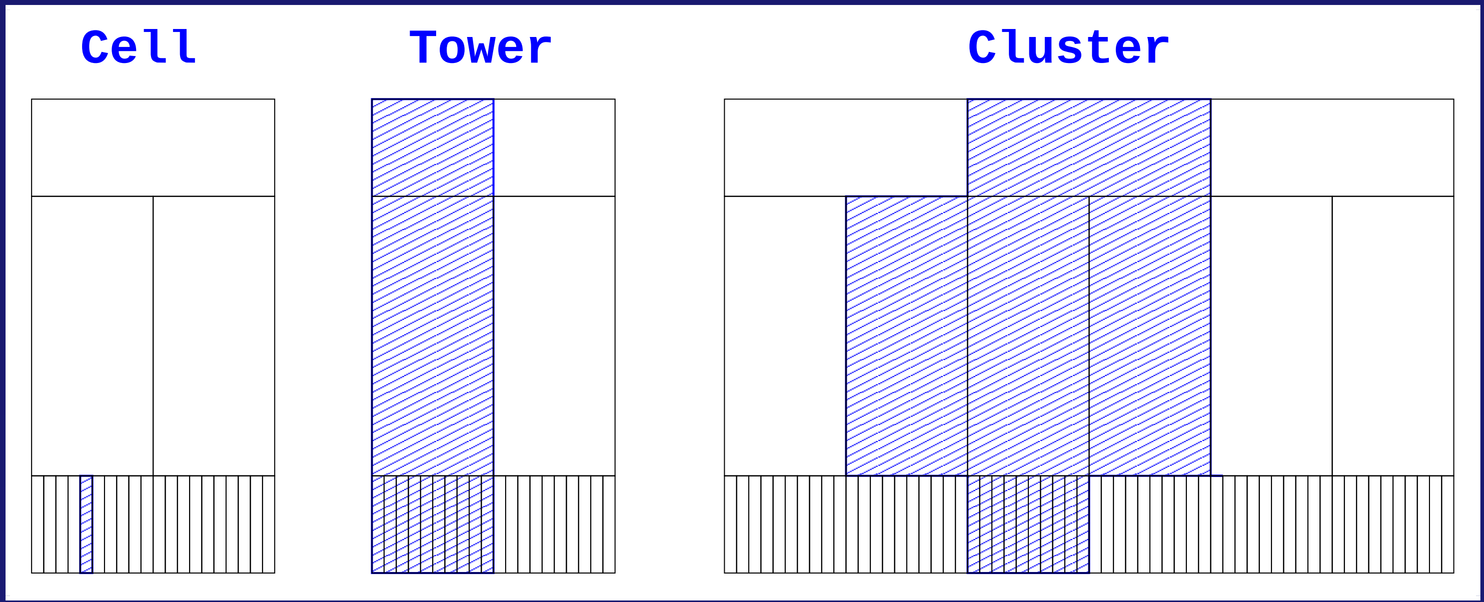

- A tower is a group of cells (or even a group of fractions of cells) in a fixed $\Delta\eta \times \Delta\phi$ grid over some or all samplings
  - contains the sum of cell (fraction) energies and the center of the grid square (η and ϕ) as members
  - in use in ATLAS are 65536 LAr EM only `LArTower`s with $\Delta\eta \times \Delta\phi = 0.025 \times 2\pi/256$
  - and 6400 `CaloTower`s including all calorimeters with with $\Delta\eta \times \Delta\phi = 0.1 \times 2\pi/64$
- A cluster is a group of cells (or even fraction of cells) formed around a seed cell
  - is the main reco object for calorimetry
  - with either a fixed size in $\Delta\eta \times \Delta\phi$ (sliding window used for electrons/photons)
  - or variable borders based on the significance of the cells (topo cluster used for hadrons/jets/MET/soft photons)
  - contains lots of data members based on weighted cell members for energy, position and shape

- Optimal filtering principle:
  - need known physics signal shape $g(t)$
  - discrete measurements (signal plus noise): $y_i = Eg_i + b_i$ in 5 samples each 25 ns
  - and autocorrelation matrix from noise runs: $B_{ij} = \langle b_i b_j \rangle - \langle b_i \rangle \langle b_j \rangle$
  - estimate amplitude E with $\tilde{E} = a^t y$ from minimization of $\chi^2(E) = (y - Eg)^t B^{-1} (y - Eg)$
  - solution is given by OF weights $a = \dfrac{B^{-1} g}{g^t B^{-1} g}$

Ionization Signal

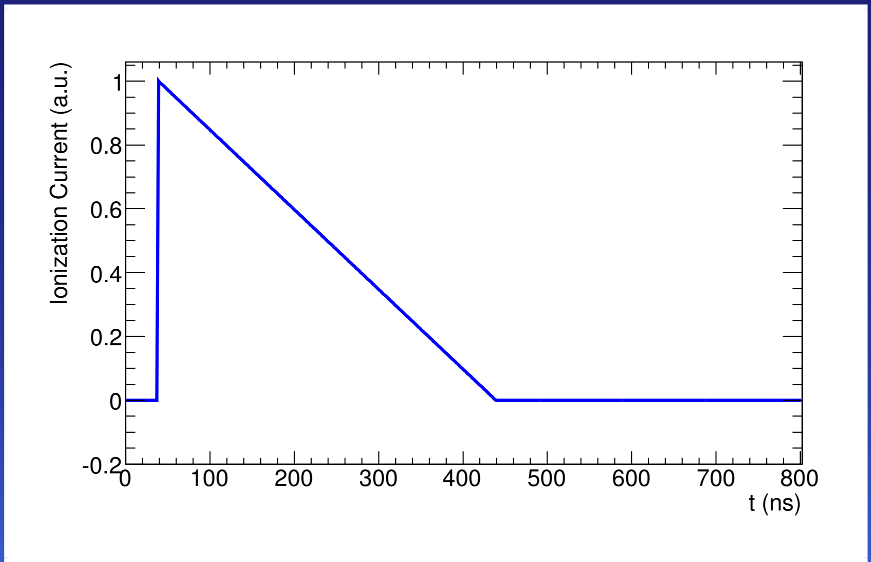

Readout Signal

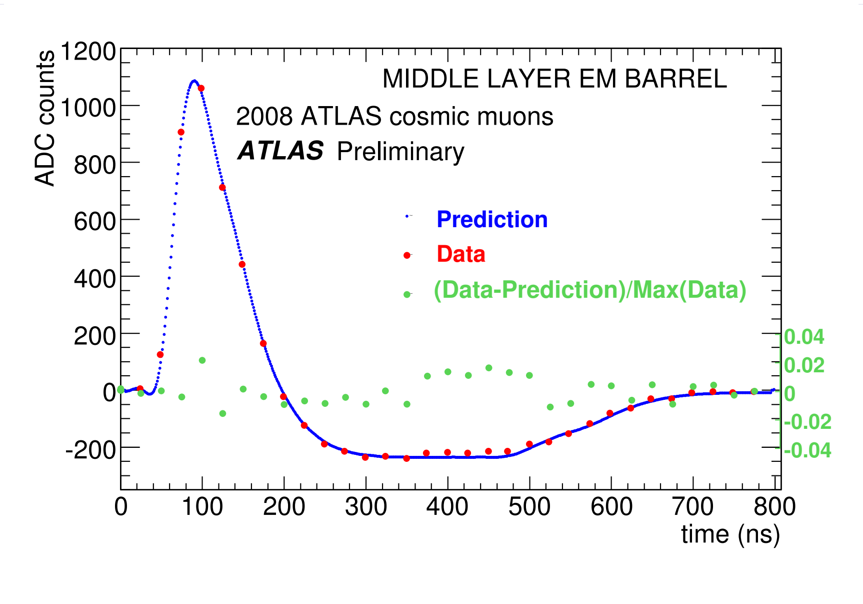

Clusters

- Cluster algorithms need to serve multiple purposes
  - suppress noise (electronics noise and pile-up)
  - keep electromagnetic showers in one cluster
  - separate multiple signals which are close by
  - work on very different sub-systems
- Plots on the right and below show large variations in η for
  - electronics noise for 2011 was set to the level of 2010 i.e. without any optimization for MinBias events ($\sim 10 - 500\,\mathrm{MeV}$)
  - total noise for 2011 for 50 ns bunch spacing and ~ 8 MinBias events per bunch crossing ($\sim 10 - 10^4\,\mathrm{MeV}$)
  - cell volume ($\sim 2 \cdot 10^4 - 3 \cdot 10^8\,,\mathrm{mm}^3$)

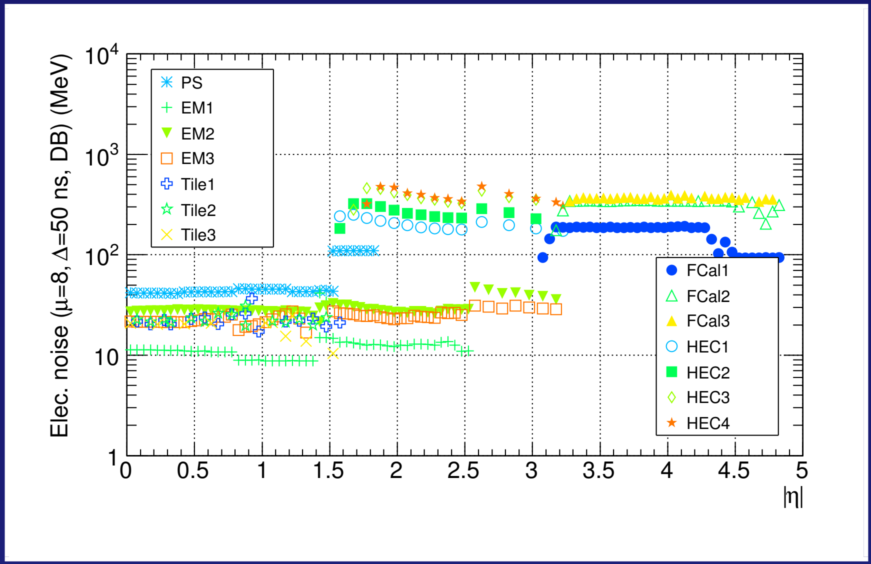

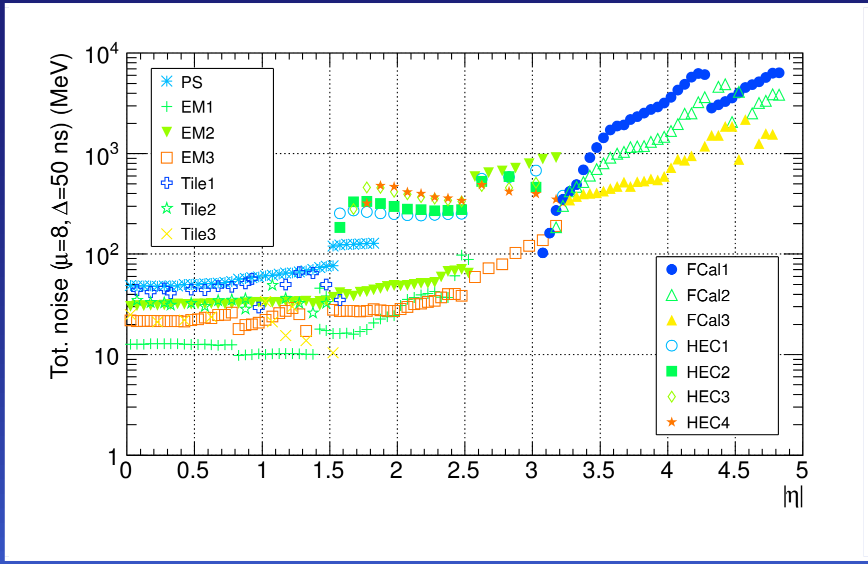

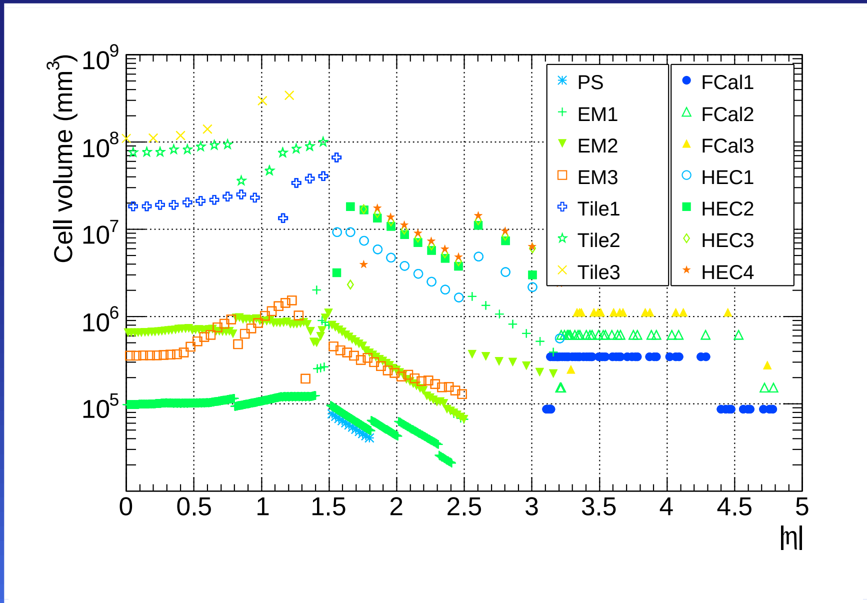

Topological Clusters

- Cluster Making
  - form clusters around seed cells with $|E_{\text{seed}}| > 4(\sigma_{\text{elec-noise}} \oplus \sigma_{\text{ pile-up-noise}})$
  - expand clusters around neighbor cells with $|E_{\text{neigh}}| > 2\sigma$
  - include perimeter cells with $|E_{\text{cell}}| > 0\sigma$
  - merge clusters if they share a neighbor cell
  - expansion is driven by neighbors in $3D$: usually 8 neighbors in the same layer ($2D$) plus cells overlapping in η and ϕ with central cell in next and previous layer (just 2 if granularity would be the same)
- Cluster Splitting
  - search for local maxima in cell energy with $E_{seed} > 500\,\text{MeV}$ in all clustered cells in EM-samplings (HAD-samplings secondary)
  - re-cluster around local maxima with same neighbor driven algorithm but no thresholds and no merging
  - cells at cluster borders are shared with energy and distance dependent weights

Topological Cluster Example

- look at di-jet MC sample including electronics noise with activity in the forward region
- plots show $|E_{\text{cell}}|$ on a color coded log-scale in MeV in the first (EM) FCal sampling for one event

$|E| > 2\,\sigma_{\text{noise}}$ $|E| > 4\,\sigma_{\text{noise}}$ $4/2/0$ topological clusters

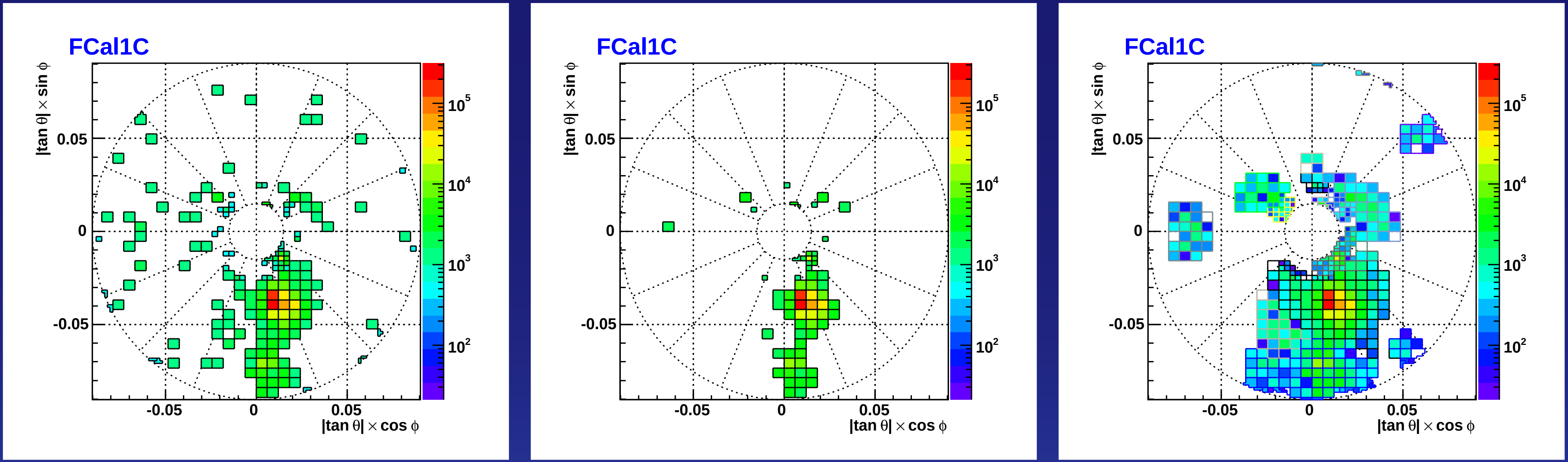

- $2\,\sigma$ cut is removing cells from the signal region
- $4\,\sigma$ cut shows seeds for the cluster maker
- after clustering all cells in the signal regions are kept
- cluster splitter finds hot spots

Topological Clusters

- Number of relevant clusters per particle
  - there can be more than 1 cluster in a cone around the original pion direction
  - but the number of relevant clusters (fraction of energy) is small
  - top plot shows energy fraction in the 3 leading clusters for charged pions vs. the pion energy in the barrel
  - bottom plot shows the same for neutral pions
  - for $E > 2\,\mathrm{GeV}$ more than 90% or the energy are in the 2 leading clusters (charged pions)
  - for neutral pions significant energy only in leading 2 clusters and only in 1 if photons can not be resolved

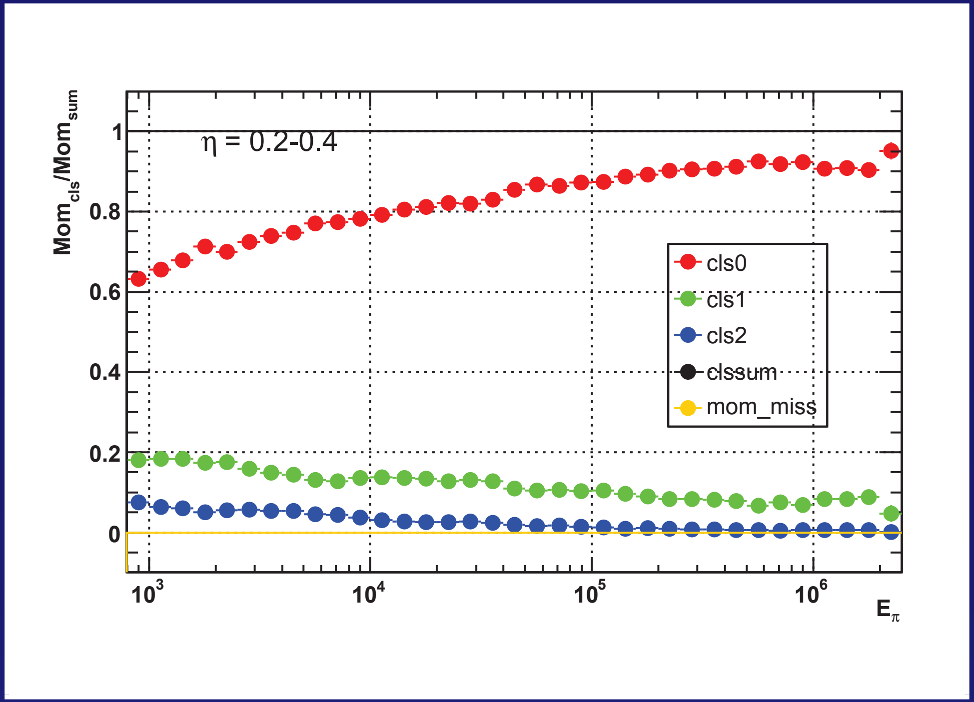

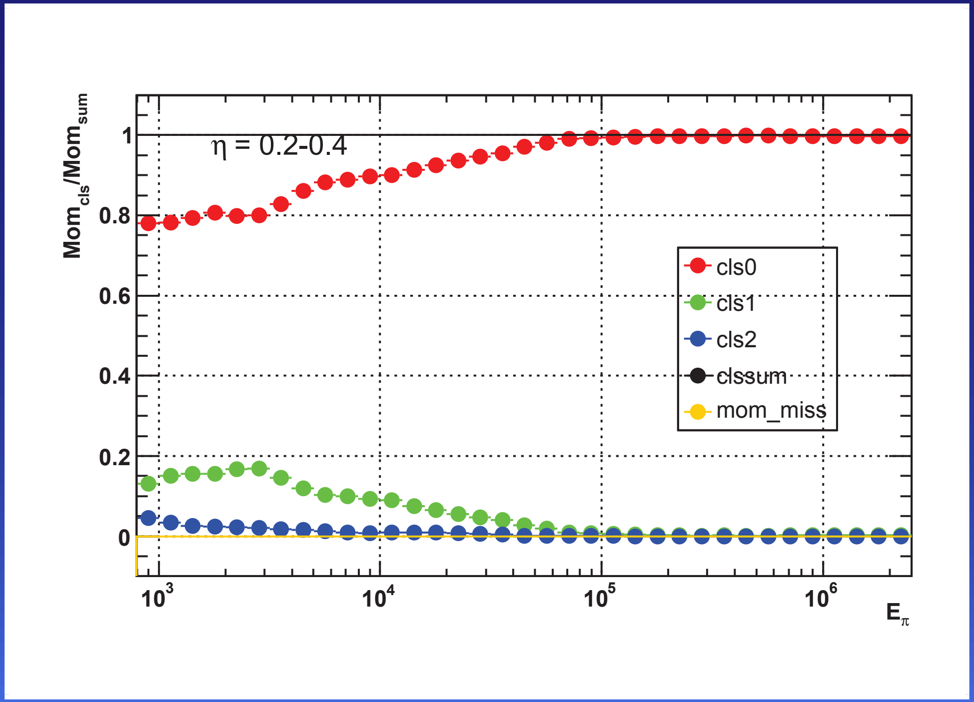

Cluster Moments

- shape variables calculated from the positive cells in a cluster
- first a principal value analysis is run on the cluster cells
  - provides centroid 3 major axes of the shower
- angles of the major axis w.r.t. IP-shower-center direction are calculated
- other shape quantities defined by moments of the form

$$\langle x^n \rangle = \frac{1}{E_{\text{norm}}} \times \sum_{\{i|E_i>0\}} E_i\, x_i^n, \text{ with}$$

$$E_{\text{norm}} = \sum_{\{i|E_i>0\}} E_i.$$

- typical choices for x: $\rho = E/V$, r, λ

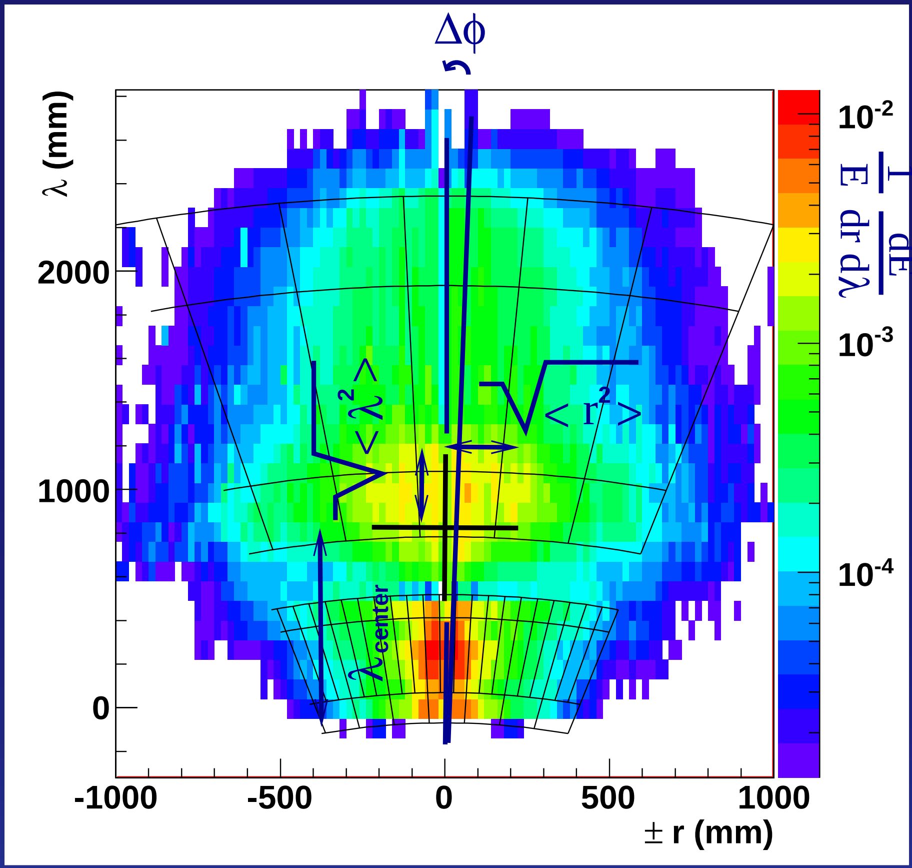

Performance ► Electrons and Photons

- high $p_\perp > 10\,\mathrm{GeV}$ isolated electrons and photons are reconstructed with fixed size LAr EM clusters in units of the middle sampling granularity of $\Delta\eta \times \Delta\phi = 0.025 \times 2\pi/256$: 3×5 for $|\eta| < 2.5$
- tracks are matched to EM clusters within a $\Delta\eta \times \Delta\phi$ window of 0.05×0.1 (large in ϕ to allow for bremsstarhlung)
- if a track match is found the object is an electron and the cluster is re-clustered in size: 3×7 (barrel); 5×5 (endcap)
- without a track match the EM cluster is called a photon candidate
- in the forward area $2.5 < |\eta| < 4.9$ topo clusters are used instead of sliding window clusters since no tracking is available here and the cluster moments of topo clusters provide good electron/pion separation power
- MC based energy corrections are applied and the absolute scale is set with $\mathrm{Z} \to \mathrm{e}^+\mathrm{e}^-$ events

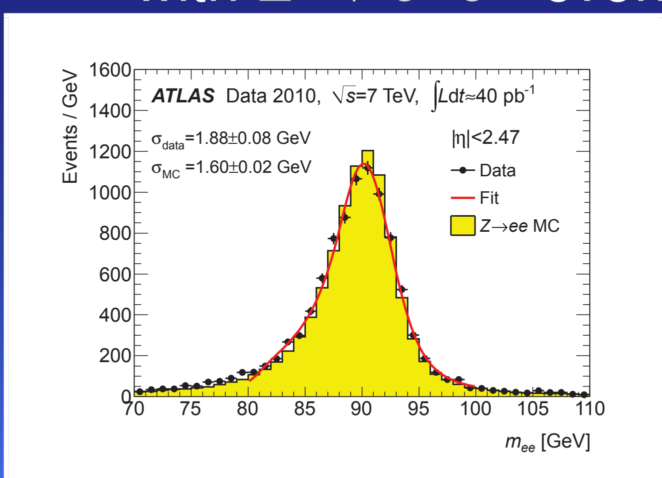

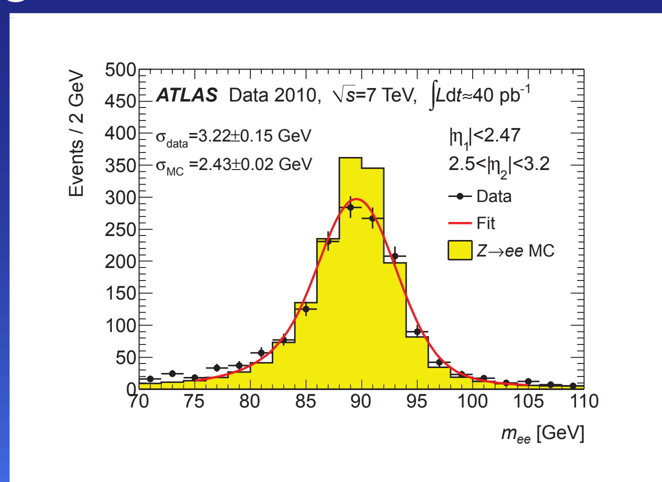

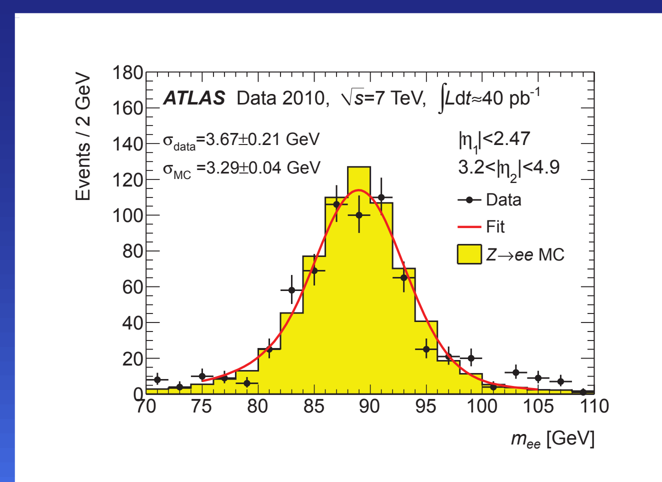

Performance ► Electrons and Photons

- low $p_\perp < 10\,\mathrm{GeV}$ photons are reconstructed with topo clusters
- note that phtons from π^0s start to merge (separation less than a cell width in the middle layer) for $E_\perp^{\pi^0} > 10\,\mathrm{GeV}$
- plots show reconstrcuted di-photon masses in various $|\eta|$ regions

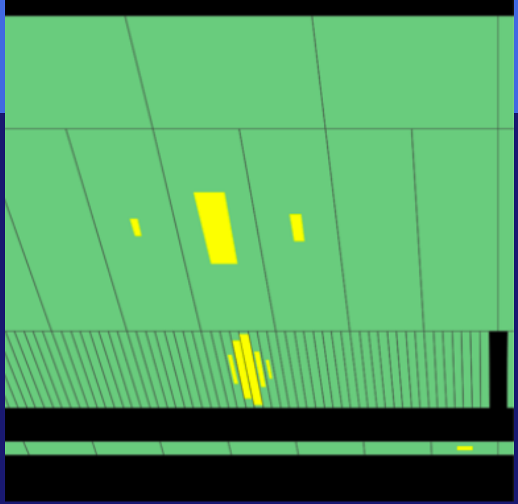

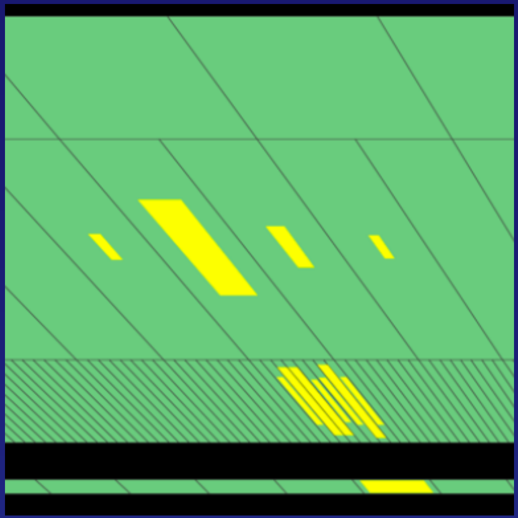

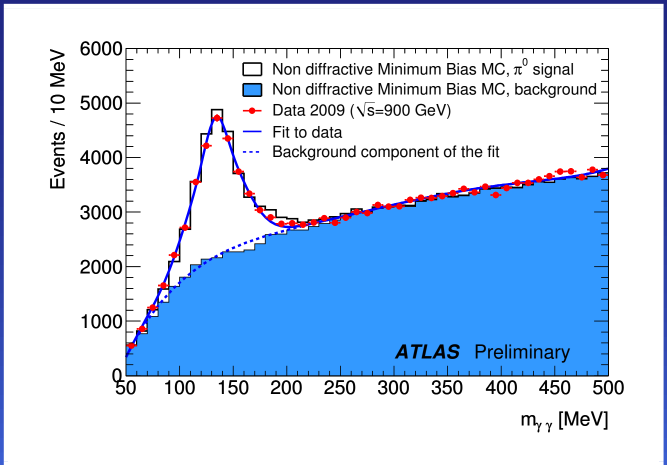

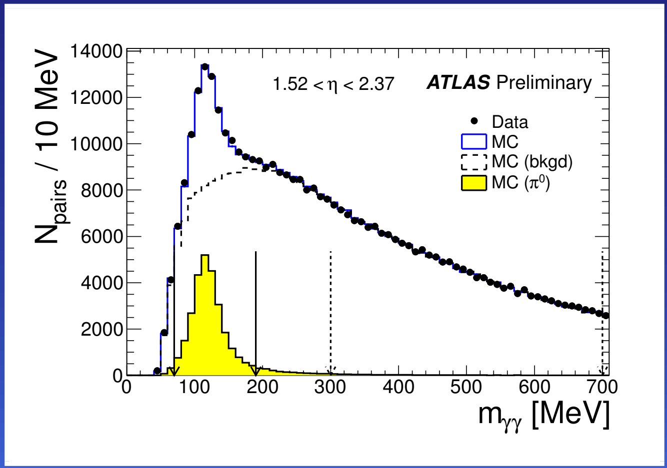

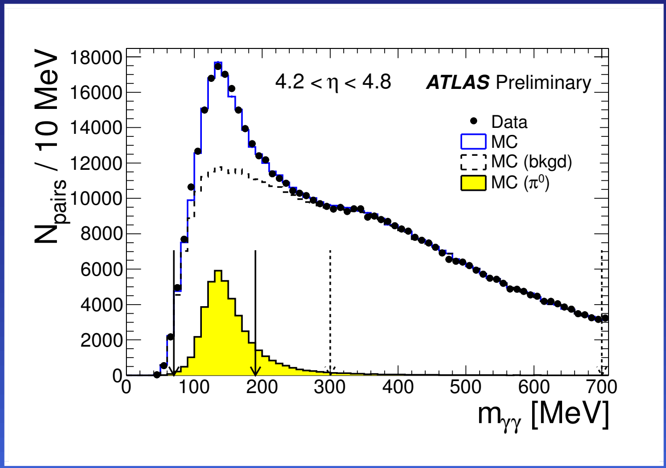

- Modern standardized jet algorithms like `SISCone` (JHEP 0705 (2007) 086), `Kt` (Nucl. Phys. B 406 (1993) 187, Phys. Rev. D 48 (1993) 3160), and `AntiKt` (JHEP 0804 (2008) 063) have been evaluated by ATLAS
  - these jets are collinear and infrared safe
  - are available in a standard `C++` library (`FastJet` by Matteo Cacciari, Gavin Salam and Gregory Soyez)
  - are seedless and iterative
- `AntiKt` in inclusive mode was found to be the most useful algorithm for ATLAS
  - `AntiKt` combines like `Kt` pairs of objects based on a $\min\left({p_T^i}^{2x}, {p_T^j}^{2x}\right)$ scaled distance metric $\Delta R_{ij}^2/R^2$ in $y-\phi$-space
  - `Kt` uses $x = 1$ and treats objects with the smallest p_T first
  - `AntiKt` uses $x = -1$ and treats objects with the largest p_T first
  - the net result is that `AntiKt`-jets are much more regular shaped in $y-\phi$ space and don't suffer from the "vacuum cleaner" effect like `Kt` making them easier to calibrate
  - ATLAS uses $R = 0.4$ and $R = 0.6$

Jet Reconstruction in ATLAS

Jets, G. Salam (p. 27)
└2. Getting the basics right
  └FastJet

Jet contours – visualised

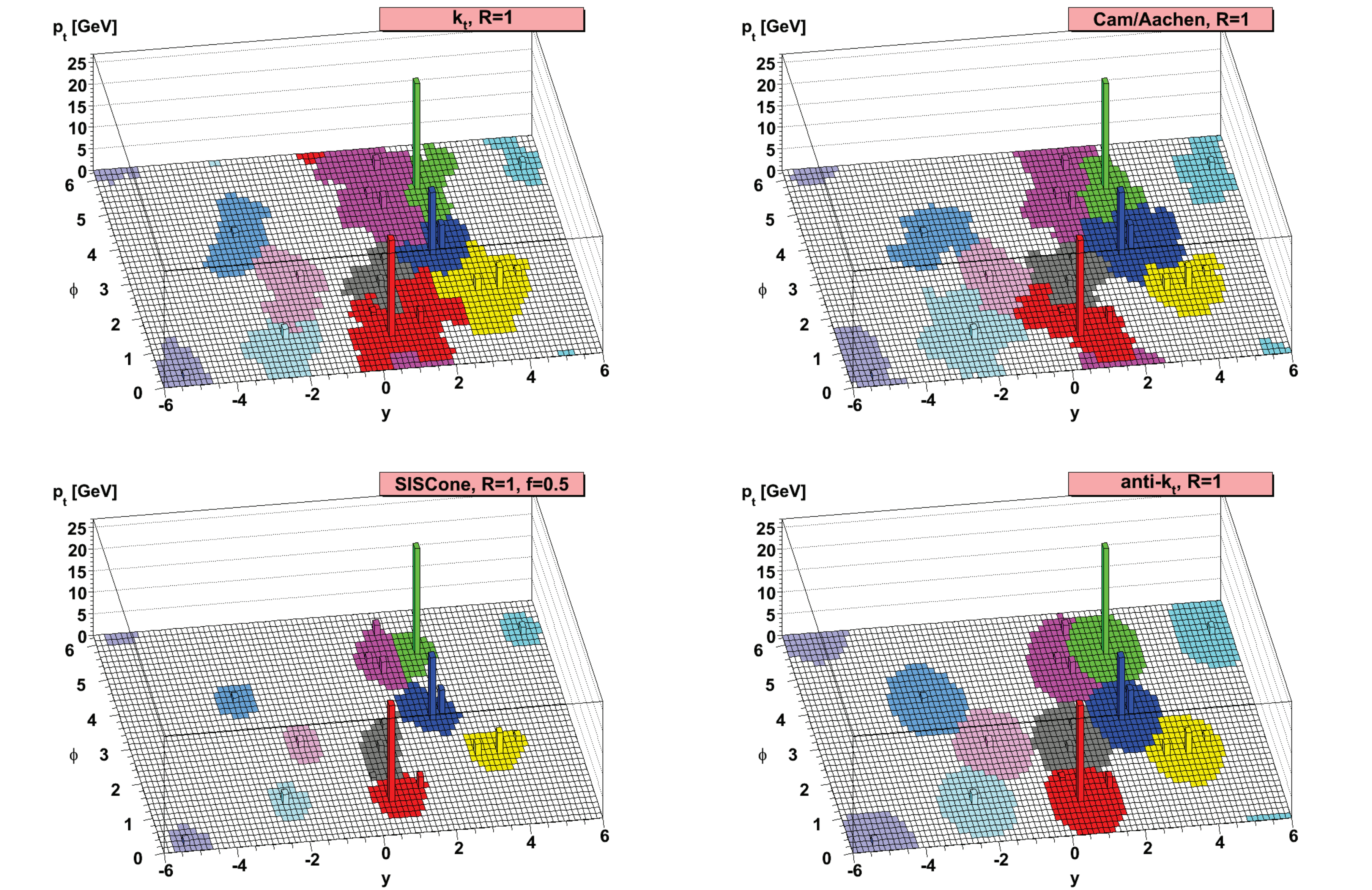

G. Salam, 2008

Jet Calibration in ATLAS

- most analyses on 2010 data used simple EM+JES scheme
  - topo clusters on EM-scale as input to jet algorithms
  - MC based correction function $f(p_\perp, |\eta|)$ to restore jet $p_\perp$ to stable hadron level
  - top plot shows correction as function of $p_\perp$ for 3 y ranges
  - middle plot shows systematic uncertainties on jet energy scale (JES) for $0.3 < |y| < 0.8$
- more sophisticated approaches exist
  - global cell weighting (GCW) applies energy-density dependent weights to all calorimeter cells
  - local hadron calibration (LCW) classifies and calibrates topo clusters as em or hadronic
  - global sequential calibration (GSW) modifies EM+JES by jets-shape based correction factors
  - bottom plot compares light-quark – gluon-jet-response for different calibration schemes
- LCW is used in ATLAS for missing transverse energy and in jets for 2011

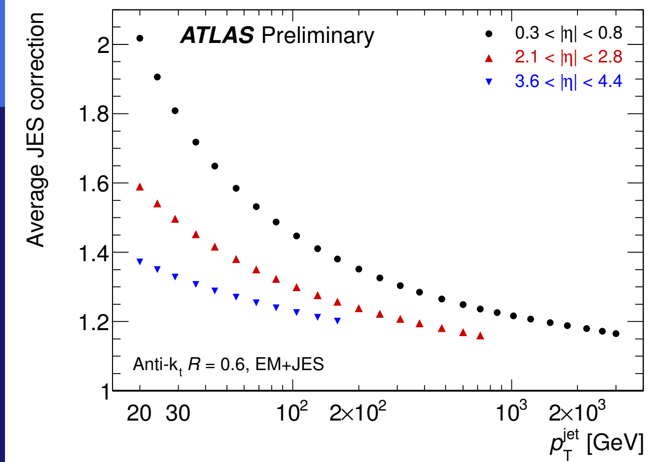

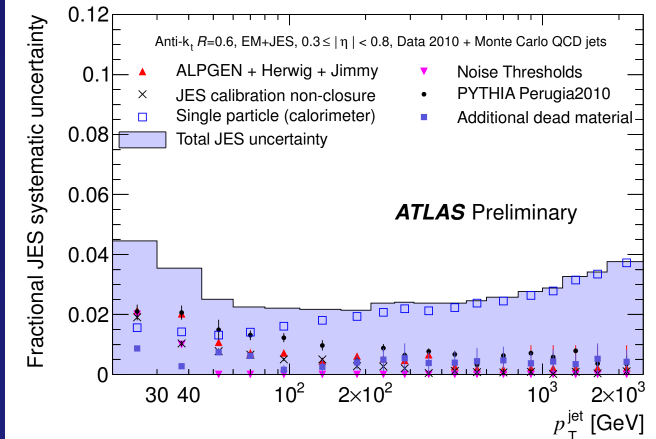

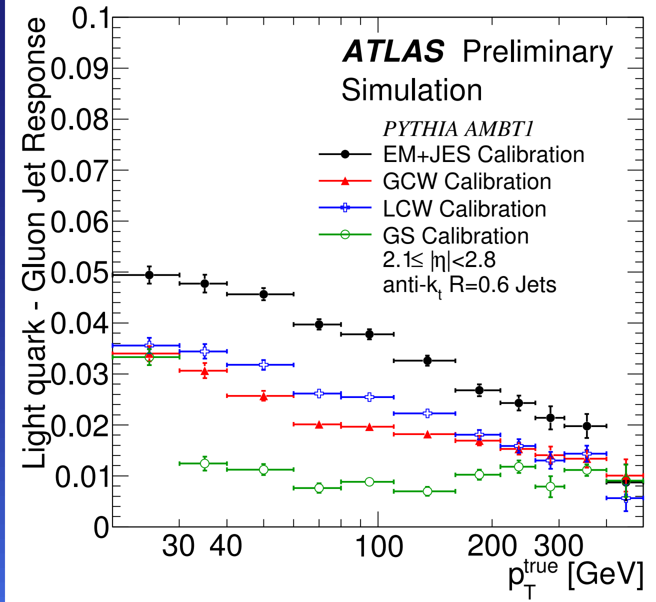

Jet Physics

- ATLAS measured the double differential cross-section in $|y|_{\max}$ and m_{12}
- bin-by-bin corrections in the observed spectra derived from simulations
- dominant exp. systematic uncertainties stem from the Jet Energy Scale uncertainty
  - $\sim 15 - 30\%$
- deviations from the QCD would indicate new physics
  - compositeness, excited quarks
- good agreement with NLO QCD predictions is observed

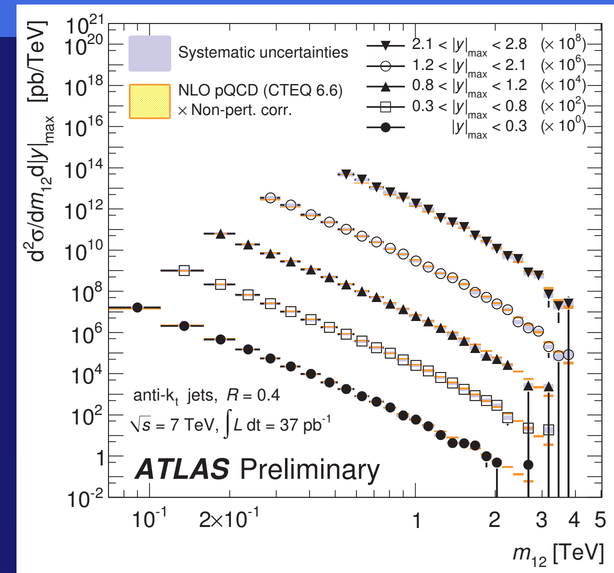

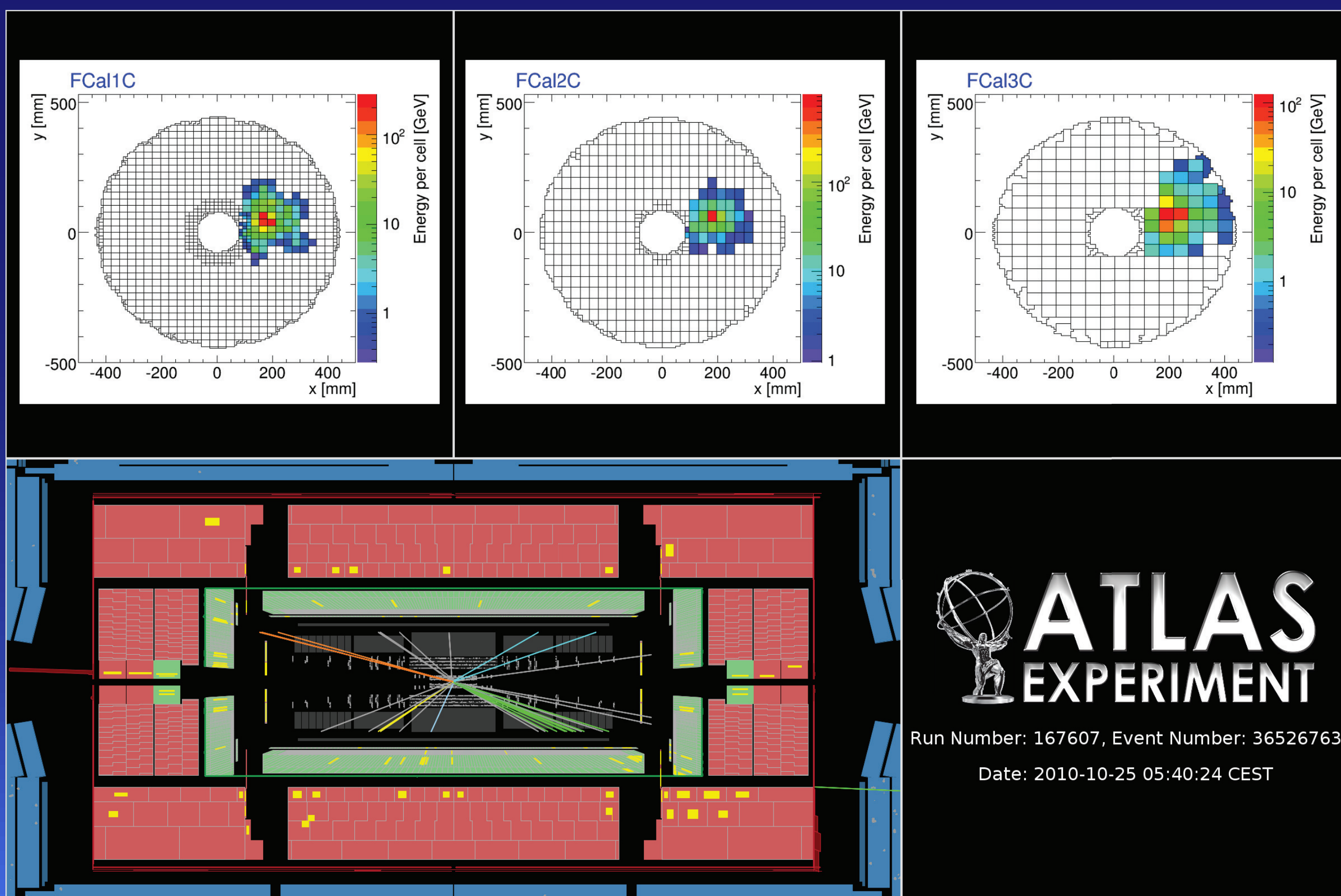

- Highest Energetic Jet in ATLAS from 2010 @ $\sqrt{s} = 7$ TeV with $E_j = 3.37$ TeV

Effects of PileUp

- In 2011 the number of minimum bias events (PileUp) per bunch crossing inreased dramatically (from essentially 0 in 2010 up to 25)
- the machine was also filled with more and more bunches
- due to the long and bi-polar shaper response (up to $\simeq 600$ ns) in the LAr calorimeters we are sensitive to PileUp from up to 24 bunch crossings id's at 25 ns nominal distances
  - the energy in the event depends on the history of bunch crossings
- about 7 nominal bunch crossing id's contribute with a positive signal; 17 with a negative signal

Shaper Response

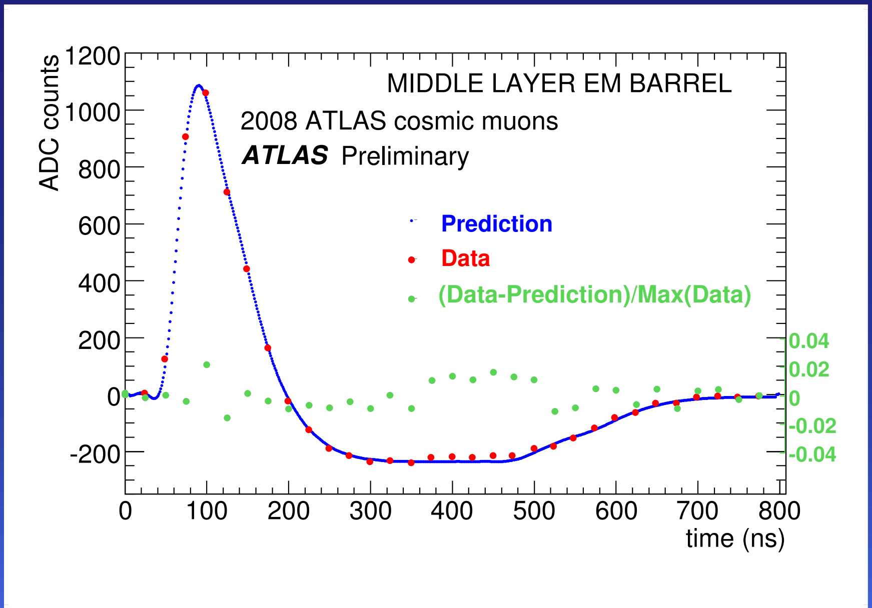

Isolation Energy

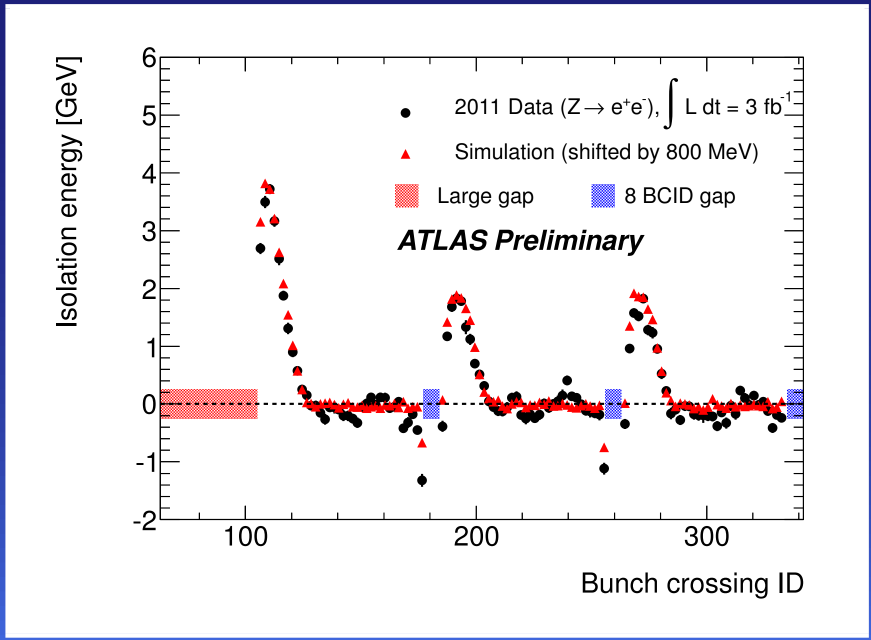

Total Noise for $\Delta t = 50$ ns and $\mu = 0, 1, 2, 5, 10, 20, 50, 100$

$\mu = 0$

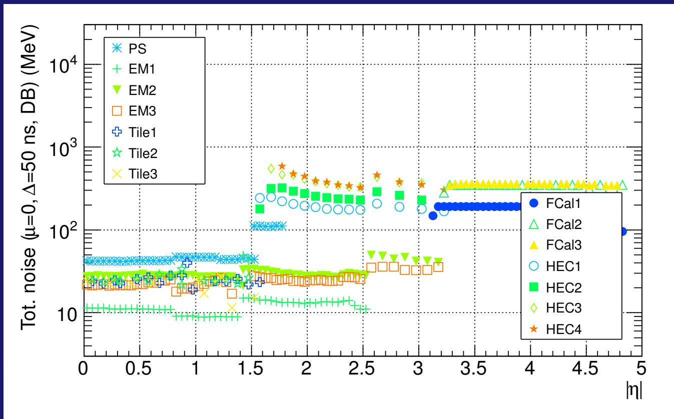

$\mu = 1$

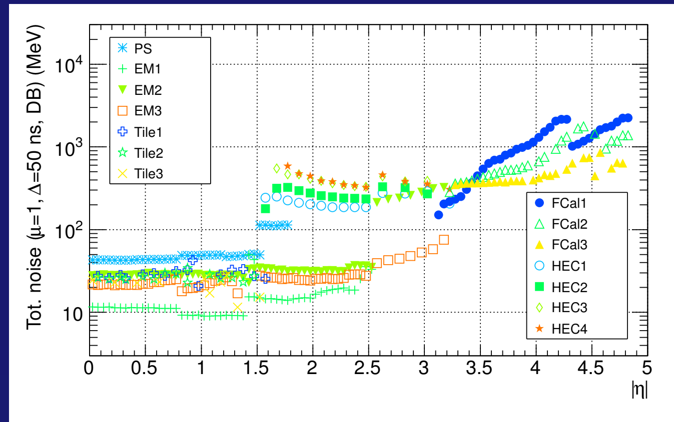

$\mu = 2$

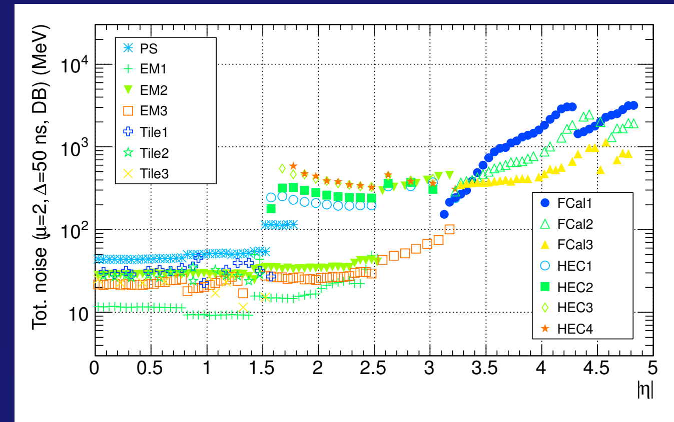

$\mu = 5$

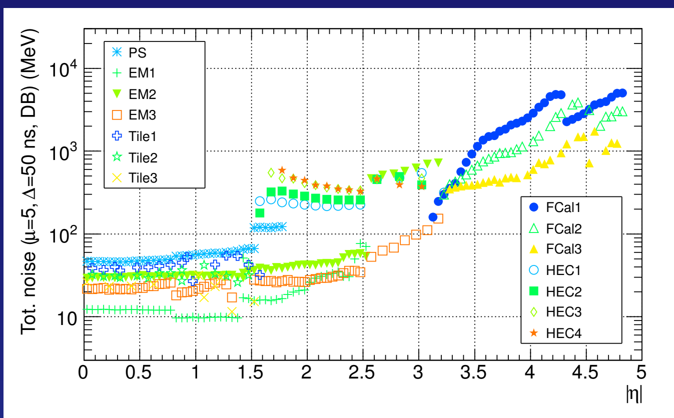

$\mu = 10$

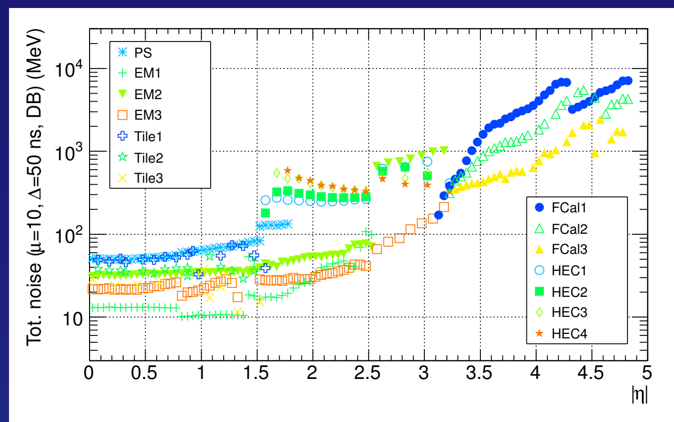

$\mu = 20$

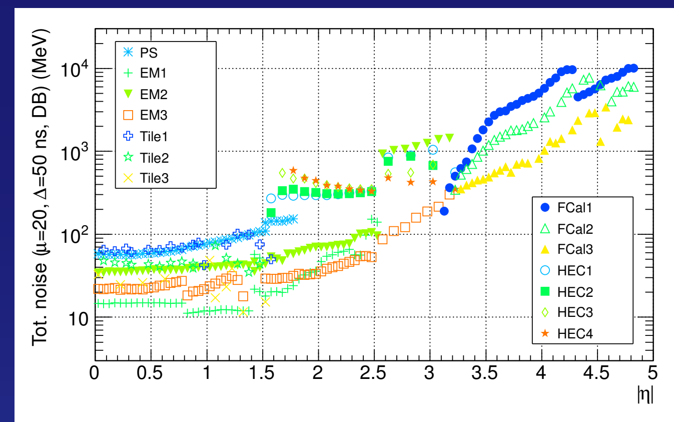

$\mu = 50$

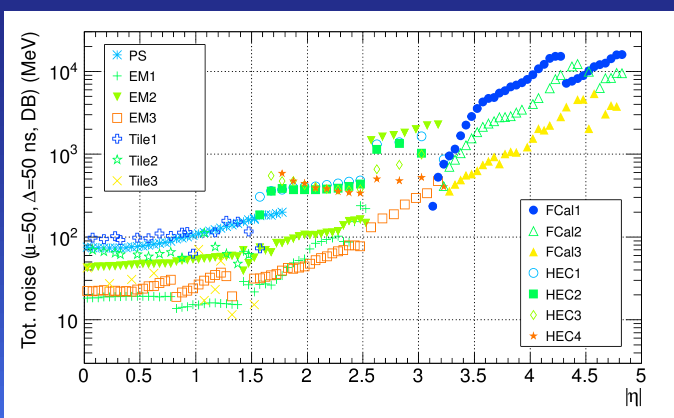

$\mu = 100$

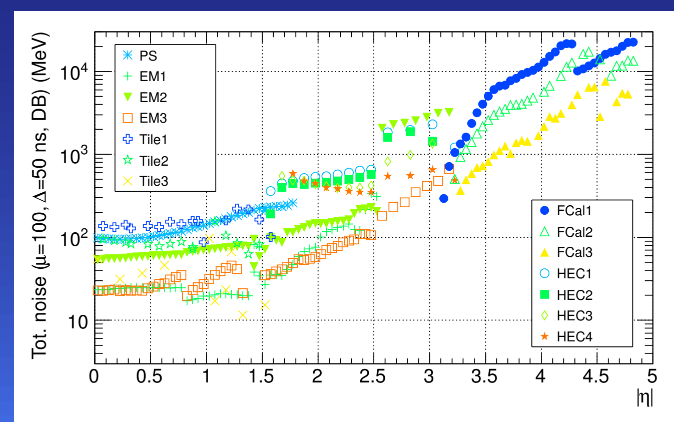

Total Noise for $\Delta t = 50$ ns and $\mu = 0, 1, 2, 5, 10, 20, 50, 100$

- Prev. slide shows total cell noise as function of $|\eta|$ for all calorimeter layers
- moderate increase $\times 2 - 5$ in the barrel from $\mu = 0$ to $\mu = 50$
- typically $\times 10$ in the endcap
- up to $\times 100$ in the forward region
- PileUp noise increases proportional to $\sqrt{\mu}$
- a 20% increase in noise means $25\times$ more clusters due to noise!
- thresholds are adjusted now for 2012 running
  - $\mu = 20$ is expected as average condition in 2012
  - aim for thresholds of 20 or 30 depending optimizations

Conclusions

- Calorimetry in ATLAS is a very diverse subject due to
  - mixture of different detector technologies
  - combined with changing conditions due to the LHC
  - and different requirements for physics (high $p_\perp$ isolated electrons/photons vs. jets)
- Topological Clusters are found to address most of above issues
  - only isolated high $p_\perp$ electrons and photons in the barrel use fixed size clusters
- Biggest challenge for 2012 is the increasing PileUp